

# Effect of H<sub>2</sub>O Vapor on NO Reduction by CO: Experimental and Kinetic Modeling Study

Sen Li,\* Xiaolin Wei, and Xiaofeng Guo

Institute of Mechanics, Chinese Academy of Sciences, No. 15 Beisihuanxi Road, Beijing 100190, People's Republic of China

**ABSTRACT:** The experiment and kinetic modeling prediction were conducted to investigate the effect of H<sub>2</sub>O vapor on NO reduction by CO. The experiment was performed in a 36-kW combustion reactor, and modeling prediction was done using the plug-flow reactor model. In the presence of H<sub>2</sub>O, the formation of free-radical H is conducive to NO reduction. H<sub>2</sub>O has a complex effect on NO emission: at  $T < 1100$  °C, NO emission decreases with the increase of H<sub>2</sub>O content and temperature, the reaction pathway of NO reduction is  $\text{NO} \rightarrow \text{HNO} \rightarrow \text{NH} \rightarrow \text{N}_2\text{O} \rightarrow \text{N}_2$ , and the controlling factors of NO reduction are temperature and H<sub>2</sub>O concentration; at  $1100$  °C  $< T < 1400$  °C, NO emission decreases as the H<sub>2</sub>O content increases and remains constant with the change of temperature at  $[\text{H}_2\text{O}] < 1.0\%$ , NO reduction depends on H<sub>2</sub>O concentration rather than temperature, and increasing H<sub>2</sub>O concentration makes free-radical H reach high equilibrium concentration; at  $T > 1400$  °C, the effects of H<sub>2</sub>O content and temperature on NO emission at  $[\text{H}_2\text{O}] < 1.0\%$  are similar to that at  $T < 1100$  °C, NO emission increases with H<sub>2</sub>O content but decreases with temperature at  $[\text{H}_2\text{O}] > 1\%$ , NO reduction depends on the combined effects of H and CO.

## 1. INTRODUCTION

Emissions of nitrogen oxides (NO<sub>x</sub>) are of great concern because of their impacts on the environment, including acid rain and photochemical smog formation. NO<sub>x</sub> is major combustion-generated pollutant from fossil fuel combustion.<sup>1</sup> The most practical and convenient method for removing nitric oxide (NO) is to use unburnt compounds such as carbon monoxide (CO), hydrogen, and hydrocarbons as reducing agents in a flame.<sup>2</sup>

Much research has focused on NO reduction by hydrogen and hydrocarbons as reducing agent, and the research on NO reduction by CO mainly focus on catalytic reduction.<sup>2–5</sup> The use of CO as a reducing agent has advantages for NO<sub>x</sub> reduction in practical application, because of its presence in significant amounts in the combustion process. The CO oxidation is carried out by NO reduction, and NO removal is usually accomplished via reduction to form N<sub>2</sub>.<sup>5</sup> The key steps in the reaction are the breaking of the NO molecule and a subsequent oxidation of the CO. However, it is found that the NO dissociation is difficult at low temperatures. Glarborg, Rasmussen, and Mueller studied the kinetic modeling of CO/H<sub>2</sub>/H<sub>2</sub>O/NO<sub>x</sub> reaction, and it found that the concentration of water vapor has a strong effect on the CO oxidation process.<sup>6–9</sup> Musgrave<sup>10</sup> found that the addition of water vapor could increase the reaction rate of NO reduction, and the following hypothesis was made about the mechanism:



It was found that careful drying reduces the reaction rate of NO reduction, and it proved that NO reduction is dependent on the presence of water at 920 °C, and the rate was independent of CO concentration if enough CO was present.

The interaction of water vapor and CO on NO reduction is little reported. To gain a deeper understanding of the actual

reactions of NO reduction, it is necessary to identify the most important reactions and the controlling factor of NO reduction. The objective of this study is to understand the interaction of H<sub>2</sub>O vapor on NO reduction by combining flow reactor experiment and kinetic modeling.

## 2. EXPERIMENT

Experimental data used for comparison with kinetic modeling prediction was obtained from a 36-kW electrically heated reactor with a corundum tube to simulate plug flow under well-controlled reaction conditions. A schematic of the reactor can be seen in Figure 1. The inner diameter, length, and wall thickness of the corundum tube were 70 mm, 1500 mm, and 5 mm, respectively.

While in the reburning zone in the utility boiler, the residence time is ~8 s. Thus, in the study, the gas residence time in the reactor is 6–8 s, the flow rate used in both experiments and modeling is 1.4 L/min at ambient temperature, and a 600-mm reactor zone length was chosen. The length of the reaction zone can be set by adjusting the position of the sampling probe. In this work, a length of 600 mm of the reaction zone was chosen.

In the experiment, the NO, CO, and Ar gases were re-stored in gas cylinders, Ar gas was used as balance gas, and these gases were highly pure. Gas concentrations were adjusted by mass-flow controllers, and gases were mixed in a gas mixer. In order to investigate the interaction of H<sub>2</sub>O vapor and CO on NO reduction, the gas mixture went through liquid H<sub>2</sub>O contained in a bottle, the relative humidity and temperature of gas mixture at the outlet was 84% and 32 °C, respectively.

The gas was analyzed with flue gas analyzers (Ecom-J2KN) manufactured by Prism Gas Detection Pvt., Ltd. The maximum relative error for the measured species was 5%.

The reactor was heated by electrical heating shells with three temperature controllers, and the temperature profiles along the reactor were measured using an S-type thermocouple. Control of the furnace

Received: April 5, 2012

Revised: June 20, 2012

Published: June 21, 2012

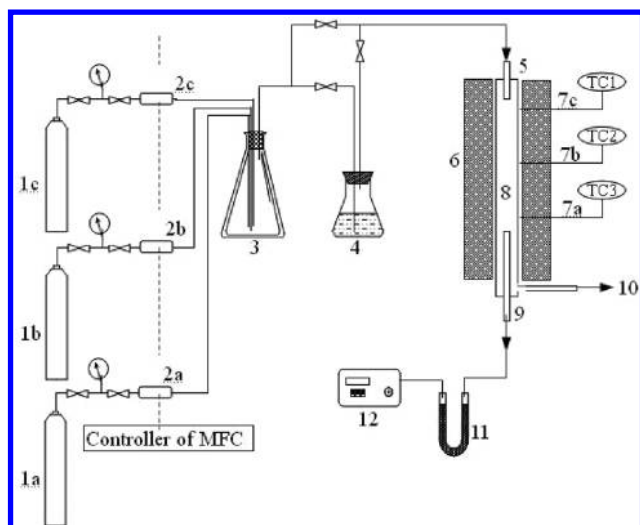


**Figure 1.** Experimental setup of the test unit. Legend: 1a–c, gas cylinders; 2a–c, mass-flow controllers; 3, gas mixer; 4, bottle containing H<sub>2</sub>O; 5, gas inlet; 6, electrically heating furnace; 7a–c, thermocouples connected to temperature controllers; 8, reaction zone; 9, quenched sampling probe; 10, flue gas outlet; 11, gas dryer; and 12, gas analyzer.

temperature was based on the temperature measurement of the corundum tube wall, and the centerline temperature profiles of the tube at different wall temperature are shown in Figure 2. The results indicate almost isothermal conditions along the reaction zone can be achieved. The tests were performed at atmospheric pressure.

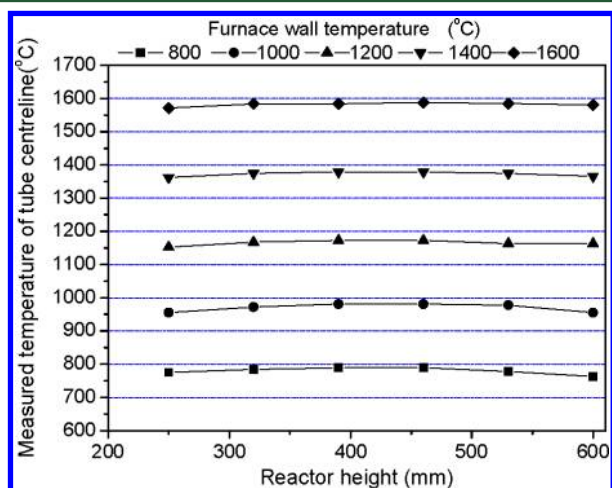


**Figure 2.** Centerline temperature profiles of the tube at different wall temperatures.

### 3. KINETIC MODELING

The above experiment is modeled as a plug-flow reactor (PFR model), and the modeling conditions are the same as those of the experiment. The PFR is simulated by Cantera software code. Cantera is an object-oriented,<sup>11,12</sup> open-source suite of software tools for reacting flow problems involves chemical kinetics, thermodynamics, and transport processes. The adopted reaction scheme to describe combustion reactions in the flames is the GRI 3.0 mechanism, which involves 53 species and 325 reactions.<sup>13,14</sup> GRI 3.0 mechanism has been extensively validated in previous studies using a variety of configurations including perfectly stirred reactors, laminar flame speeds, and

nonpremixed and partially premixed flames.<sup>15–17</sup> Therefore, GRI 3.0 mechanism can be used to model burning flames and NO<sub>x</sub> emissions.

The reaction pathway flux analysis is performed using MixMaster (a Python program that is part of the Cantera suite), which is based on a conserved scalar approach to reaction fluxes.<sup>11</sup>

## 4. RESULTS AND DISCUSSION

In the experiment, the initial concentration of H<sub>2</sub>O vapor in gas mixture has a great effect on NO emission, but the precise and stable adjustment of H<sub>2</sub>O vapor is very difficult when the concentration is <0.5%. In the study, in order to ensure the accuracy of the experimental result, the concentration of H<sub>2</sub>O vapor in gas mixture was kept constant (4.0%) in the experiment, and the effect of H<sub>2</sub>O vapor on NO emission was investigated by the kinetic reaction modeling, using a validated PFR model.

### 4.1. Influence of Temperature and H<sub>2</sub>O Vapor on NO Reduction by CO. Figure 3 shows the comparison of

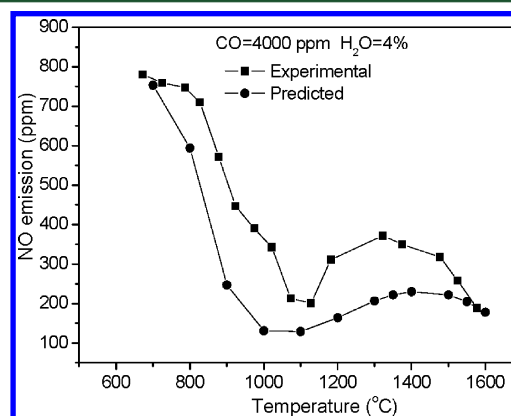


**Figure 3.** Comparison of experimental and modeling NO emission at 600–1600 °C.

experimental and modeling NO emission at 600–1600 °C. The results show that, with the increase of temperature, NO emission rapidly decreases at 800 °C < T < 1100 °C, increases at 1100 °C < T < 1400 °C, and then decreases at T > 1400 °C. In the experiment, the initial temperature of gas mixture is ambient temperature, the reaction is delayed by heating when gas mixture entered reactor, and then there is a difference between the predicted and measured values of NO emission in Figure 3. Although there is a difference between the predicted and measured values, the change trends of the predicted and measured NO emission with the increase of temperature are in good agreement. Therefore, PFR kinetic reaction modeling can be used to analyze the influencing mechanism of NO reduction by CO.

In order to investigate the influence of H<sub>2</sub>O vapor on NO emission, a PFR model is used to predict NO reduction by CO at [H<sub>2</sub>O] = 0–8%, and the results are shown in Figure 4. The results show that the effect of H<sub>2</sub>O vapor on NO reduction is complex: at T < 1100 °C, NO emission rapidly decreases with the increase of initial H<sub>2</sub>O concentration and temperature when H<sub>2</sub>O is <0.6%, but NO reduction is not noticeable with the increase of H<sub>2</sub>O content when [H<sub>2</sub>O] > 0.6%; at T > 1100 °C and [H<sub>2</sub>O] < 1.0%, NO emission almost keep constant in the range of 1100–1400 °C at a given H<sub>2</sub>O concentration, it

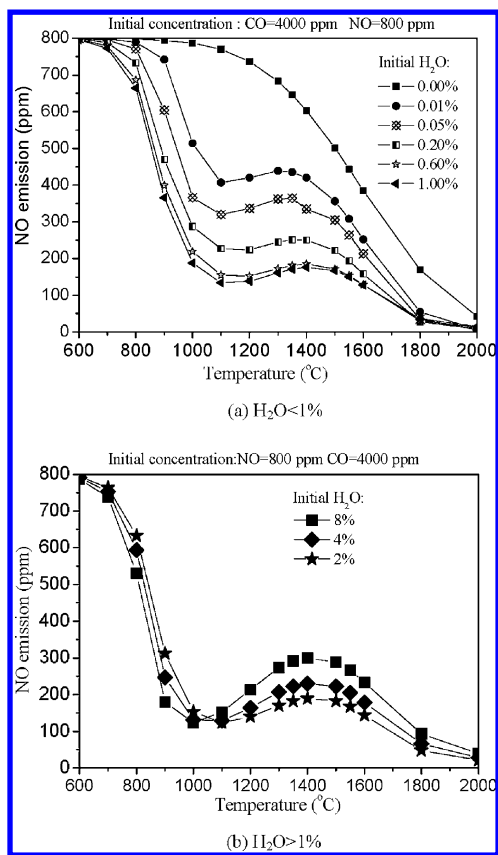


Figure 4. Modeling prediction of the effect of H<sub>2</sub>O content on NO emission by CO.

gradually decreases with the increase of temperature at  $T > 1400$  °C, and decreases with the increase of H<sub>2</sub>O concentration; at  $T > 1100$  °C and  $[H_2O] > 1.0\%$ , with the increase of temperature, NO emission slightly increases, reaches a peak value at  $T = 1400$  °C, and then begins to decrease at  $T > 1400$  °C, and increasing H<sub>2</sub>O concentration makes the NO emission increase (see Figure 4b).

In order to systematically investigate the interaction of the concentrations of H<sub>2</sub>O, NO, and CO on NO reduction, NO emission is predicted at different initial concentrations of H<sub>2</sub>O, NO, and CO at  $T > 1100$  °C. Since the simulated results show that the change trends of NO emission with the initial concentrations of H<sub>2</sub>O, NO, and CO are similar at different temperatures ( $T > 1100$  °C), the result of NO emission at  $T = 1400$  °C is only presented in Figure 5. The results indicate that there is minimal NO emission at  $[H_2O] = 1\%$ , and increasing CO makes the NO emissions decrease at different initial concentrations of CO and NO.

**4.2. Mechanism Analysis of H<sub>2</sub>O Vapor on NO Reduction.** The above experimental and simulated results indicate that the initial H<sub>2</sub>O concentration has a great and complex effect on NO emission. In order to analyze the mechanisms of NO reduction, the reaction pathway flux analysis is performed using MixMaster, and the integral path analysis is based on a conserved scalar approach to reaction fluxes.<sup>7</sup>

In order to analyze the interaction of H<sub>2</sub>O vapor and CO on NO reduction, the reaction mechanism of NO reduction by CO in the absence of H<sub>2</sub>O is first investigated. Figure 6 illustrates the detailed reaction pathway diagram for N- and C-containing species at  $L = 150$  mm (the position from the inlet,

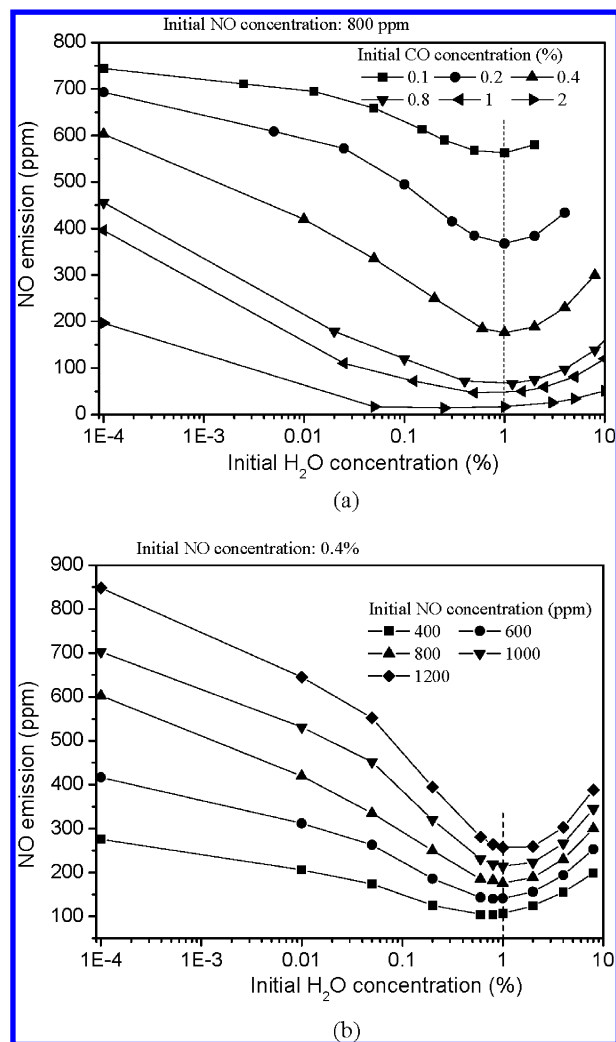


Figure 5. Modeling prediction of the effect of the initial concentrations of H<sub>2</sub>O, CO, and NO on NO emission at  $T = 1400$  °C.

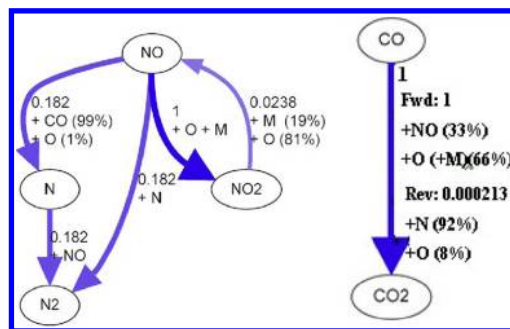
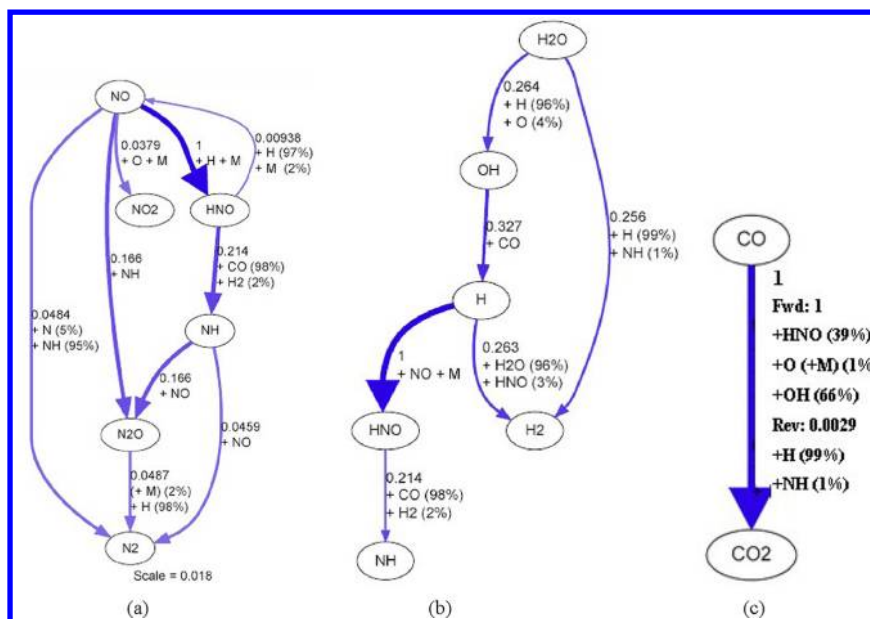


Figure 6. Reaction pathway diagrams for N- and C-containing species at  $[CO] = 4000$  ppm,  $[H_2O] = 0\%$ ,  $T = 1400$  °C, and  $L = 150$  mm.

see Figure 1), where the number (e.g., 0.182) on the arrows represent the relative element reaction fluxes, the percentage (e.g., 99%) is a certain reaction contribution rate for production; “Fwd” and “Rev” respectively represent the forward reaction and reversible reaction, and the relative width of the arrows in Figure 6 indicates pathway importance. Figure 6 indicates that, in the absence of H<sub>2</sub>O, NO is reduced into N<sub>2</sub> mainly by CO, the contribution of CO to NO reduction is 99%, and CO is oxidized into CO<sub>2</sub> in the process of NO reduction by



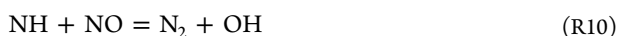
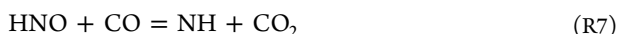
**Figure 7.** Reaction pathway diagrams for N-, H-, and C-containing species in the presence of H<sub>2</sub>O. The initial concentrations are given as follows: [CO] = 4000 ppm, [H<sub>2</sub>O] = 0.2%. T = 850 °C, and L = 150 mm.

CO. The detailed pathways of NO reduction and CO oxidation are as follows:

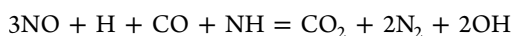


Increasing the temperature is conducive to the forward reactions of reactions R3 and R4, and then NO emission monotonically decreases with temperature (see Figure 4a). However, since reaction R5 is very slow in the absence of H<sub>2</sub>O,<sup>18</sup> it is not conducive to the forward reaction of reaction R4, and then NO reduction slows in the absence of H<sub>2</sub>O when the temperature is <1100 °C (see Figure 4a).

In the presence of H<sub>2</sub>O vapor and at T < 1100 °C, the experimental and predicted results show that NO emission rapidly decreases as the temperature increases, and the reaction pathway is investigated at T = 850 °C. Figure 7 shows the reaction pathway diagrams for N-, H-, and C-containing species in the presence of H<sub>2</sub>O at T = 850 °C, and it indicates that H plays a great role in NO reduction, and the detailed pathways of NO reduction are as follows:



Net:



The reaction pathway of NO reduction is NO → HNO → NH → N<sub>2</sub>O → N<sub>2</sub>, and reactions R6–R9 are the crucial steps in the NO reduction pathways where free-radical H plays a key role. As known from the reaction pathway of H- and C-

containing species, the free-radical H originates from the following reactions:



The role of H<sub>2</sub>O in NO reduction is very complex for the formation of free-radical H. High H<sub>2</sub>O concentration may reduce free-radical H and produce more free-radical OH through reaction R11, but high OH content is conducive to free-radical H formation through reaction R12. When the temperature and H<sub>2</sub>O content are, respectively, <1100 °C and 1.0%, the controlling factors of NO reduction are temperature and H<sub>2</sub>O concentration.

Figure 8 shows the variation of free-radical H concentration with initial H<sub>2</sub>O vapor concentration and temperature at L =

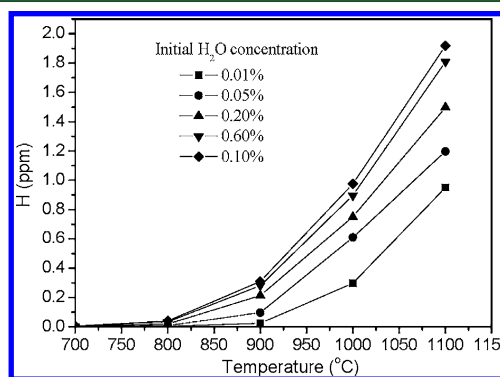


**Figure 8.** Modeling prediction of the influence of temperature and H<sub>2</sub>O on the free-radical concentration of H at [CO] = 4000 ppm and L = 150 mm.

150 mm and T < 1100 °C. As known from Figure 8, when the temperature is >900 °C, free-radical H concentration rapidly increases as the temperature increases. When the H<sub>2</sub>O concentration is low, the CO oxidation rate is low,<sup>17</sup> the concentrations of CO and CO<sub>2</sub> in reaction R12 do not reach

equilibrium, increasing the temperature and H<sub>2</sub>O concentration can increase the free-radical concentrations of H (see Figure 8), and then NO emission rapidly decreases as the temperature increases at  $T < 1100\text{ }^{\circ}\text{C}$  (see Figure 4). At  $[\text{H}_2\text{O}] > 0.6\%$ , the increase of free-radical H concentration with H<sub>2</sub>O vapor concentration is not noticeable at a given temperature (see Figure 8), and thus the change of NO emission with initial H<sub>2</sub>O vapor concentration is slight at  $T < 1100\text{ }^{\circ}\text{C}$  (see Figure 4b).

At  $[\text{H}_2\text{O}] < 1.0\%$  and  $1100\text{ }^{\circ}\text{C} < T < 1400\text{ }^{\circ}\text{C}$ , the pathway of NO reduction is similar to that at  $T < 1100\text{ }^{\circ}\text{C}$  (see Figure 7), but the controlling factor of NO reduction is only the H<sub>2</sub>O concentration, instead of temperature. At  $1100\text{ }^{\circ}\text{C} < T < 1400\text{ }^{\circ}\text{C}$ , the free-radical concentrations of H and OH in reactions R11 and R12 can rapidly reach equilibrium in the temperature range at a given H<sub>2</sub>O content, and the reaction temperature has little effect on NO reduction through reactions R6–R10. However, increasing the H<sub>2</sub>O concentration makes the amount of free-radical H reach high equilibrium concentrations through reactions R11 and R12, and NO can be effectively reduced through reactions R6–R10. Therefore, NO emission almost remains constant with the increase of temperature, and decreases as the H<sub>2</sub>O content at  $1100\text{ }^{\circ}\text{C} < T < 1400\text{ }^{\circ}\text{C}$  and  $[\text{H}_2\text{O}] < 1.0\%$  (see Figure 4a).

Figure 9 shows the reaction pathway of N-containing species at  $T = 1600\text{ }^{\circ}\text{C}$ , it indicates that there are two pathways of NO

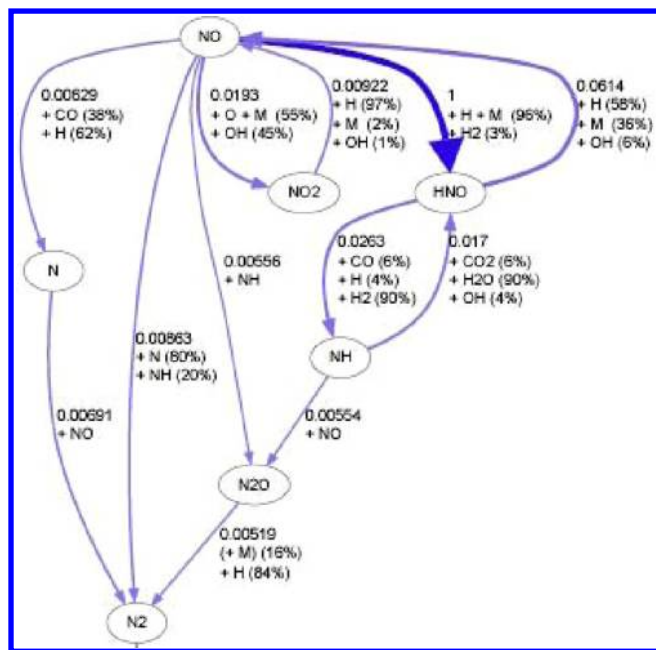
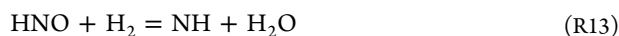


Figure 9. Reaction pathway diagrams for N-containing species at  $[\text{CO}] = 4000\text{ ppm}$ ,  $[\text{H}_2\text{O}] = 0.2\%$ ,  $T = 1600\text{ }^{\circ}\text{C}$ , and  $L = 150\text{ mm}$ .

reduction, the first pathway is similar to reactions R6–R10, but reaction R6 is replaced by the following reaction:



The other pathway is as follows:



Therefore, the two NO reduction pathways are: (1)  $\text{NO} \rightarrow \text{HNO} \rightarrow \text{NH} \rightarrow \text{N}_2\text{O} \rightarrow \text{N}_2$  and (2)  $\text{NO} \rightarrow \text{N} \rightarrow \text{N}_2$ . The pathways of NO reduction indicate that both H and CO have a high capability of NO reduction, and CO can be directly oxidized to reduce NO via reaction R15 at high temperature. Reaction R14 is very important, with regard to the NO reduction path: high levels of OH can promote NO formation, but H can easily reduce NO to N<sub>2</sub>. Thus, the appropriate concentrations of H and OH are very important for NO reduction.<sup>19</sup> High temperature can increase the reaction rates of R14–R16; therefore, NO emission decreases with temperature when the temperature is  $>1400\text{ }^{\circ}\text{C}$  (see Figure 4).

Figure 10 shows the effect of H<sub>2</sub>O concentration on free-radical H content at  $[\text{CO}] = 4000\text{ ppm}$  and  $T = 1400\text{ }^{\circ}\text{C}$ , and it

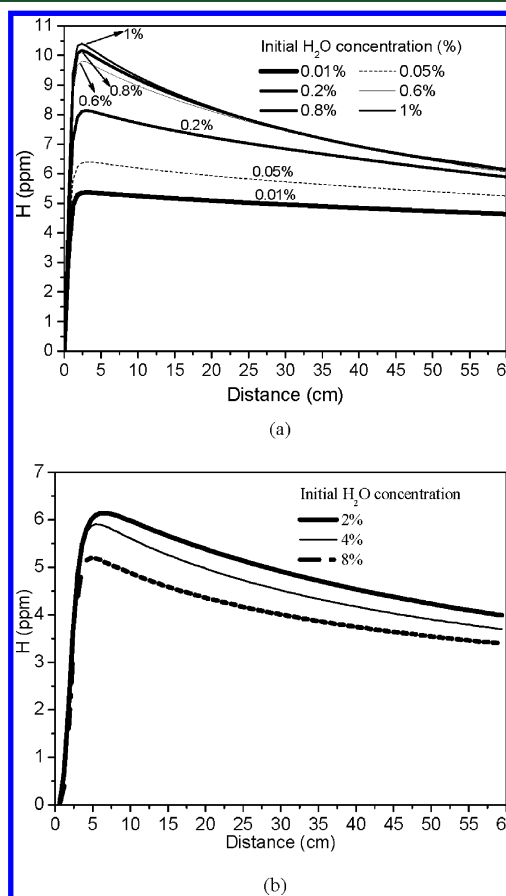


Figure 10. Effect of H<sub>2</sub>O concentration on free-radical H content at  $[\text{CO}] = 4000\text{ ppm}$  and  $T = 1400\text{ }^{\circ}\text{C}$ .

indicates that the free-radical H concentration increases as the initial H<sub>2</sub>O concentration increases at  $[\text{H}_2\text{O}] < 1.0\%$ , but it decreases as the initial H<sub>2</sub>O concentration increases at  $[\text{H}_2\text{O}] > 1.0\%$ . At  $[\text{H}_2\text{O}] < 1.0\%$  and  $T > 1100\text{ }^{\circ}\text{C}$ , the controlling factor of NO reduction is only H<sub>2</sub>O concentration; the free-radical concentrations of H and OH in reactions R11 and R12 can rapidly reach equilibrium in the temperature range at a given H<sub>2</sub>O content. Increasing the H<sub>2</sub>O concentration makes the amount of free-radical H reach high equilibrium concentrations through reactions R11 and R12, and NO can be effectively reduced through reactions R6–R10 (see Figure 5). However, at  $\text{H}_2\text{O} > 1.0\%$  and  $T > 1100\text{ }^{\circ}\text{C}$ , increasing H<sub>2</sub>O concentration is conducive to the backward reaction of reaction R13 (see Figure 9), increasing H<sub>2</sub>O can reduce free-radical H by reaction R11

(see Figure 10), and high H<sub>2</sub>O concentration ([H<sub>2</sub>O] > 1.0%) is not conducive to NO reduction at  $T > 1100$  °C (see Figures 4 and 5). Therefore, there is minimal NO emission at [H<sub>2</sub>O] = 1% in Figure 5.

The normalized sensitivity of NO concentration toward reactions are calculated, the sensitivity analysis coefficients are obtained through perturbation of the pre-exponential factor  $A$  in the Arrhenius equation of reaction, and the normalized sensitivity coefficient ( $S_i$ ) is defined as

$$S_i = \frac{\partial \ln c}{\partial \ln k_i} \quad (1)$$

where  $c$  is the NO concentration, and  $k_i$  is the pre-exponential factor  $A$  in the Arrhenius equation of reaction  $i$ . The value of the sensitivity coefficient indicates a positive or negative influence on  $c$  by  $k_i$ : a positive value means that the value of  $c$  increases as  $k_i$  increases, and a negative value means that the value of  $c$  decreases as  $k_i$  increases. The reason for the high value of this coefficient is that the reaction is the key chain-branching step and strongly promotes NO oxidation.

As known from Figure 11, the normalized sensitivity coefficients of reactions R6, R13, and R15 are the top three,

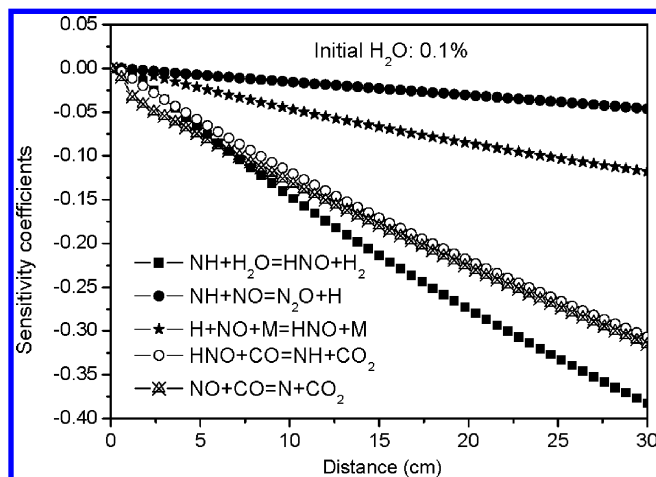


**Figure 11.** Sensitivity of NO concentrations toward the most important reactions at [CO] = 4000 ppm, [NO] = 800 ppm, and  $T = 1400$  °C.

which means that the three reactions are most important for NO reduction, and the CO, H<sub>2</sub>O, and free-radical H contents are important for NO reduction. In reactions R11 and R12, at a given temperature, free-radical H formation depends on the concentrations of H<sub>2</sub>O and CO. When the H<sub>2</sub>O content is too low, the controlling factor of free-radical H formation is the H<sub>2</sub>O concentration, and increasing the H<sub>2</sub>O vapor concentration can increase the H concentration, which is conducive to NO reduction; when the H<sub>2</sub>O vapor concentration is too high, the controlling factor of free-radical H formation is CO concentration, and only increasing the CO concentration can increase the H concentration at high H<sub>2</sub>O content. At [H<sub>2</sub>O] > 1.0% and  $1100$  °C <  $T < 1400$  °C, NO reduction is mainly dependent on free-radical H content in the reaction pathways. At a given CO content, increasing the temperature can reduce the H concentration via reaction R11, and it makes the NO reduction decrease.

At [H<sub>2</sub>O] > 1% and  $T > 1400$  °C, NO reduction depends on the free-radical H and CO content. CO can be directly oxidized

to reduce NO via reaction R15 at high temperature, and high temperature can increase the reaction rates of reactions R14–R16, and, thus, NO emission decreases with temperature at  $T > 1400$  °C. Therefore, for practical application of NO reduction in a pulverized-coal-fired furnace, when air staging or reburning is used to reduce NO emission, the temperature of the reduction should be <1400 °C, and the H<sub>2</sub>O content should not be too high.

## 5. CONCLUSION

The effect of H<sub>2</sub>O on NO reduction by CO is complex: (1) at  $T < 1100$  °C, NO emission rapidly decreases when H<sub>2</sub>O increases from 0 to 0.60% and slightly decreases when H<sub>2</sub>O is greater than 0.6%, and NO emission rapidly decreases with the increase of temperature; (2) at  $1100$  °C <  $T < 1400$  °C, NO emission decreases as the H<sub>2</sub>O content increases and remains constant with the change of temperature at H<sub>2</sub>O < 1%, and NO emission increases with the increase of H<sub>2</sub>O concentration and temperature at H<sub>2</sub>O > 1%; (3) at  $T > 1400$  °C, the effects of H<sub>2</sub>O and temperature on NO emission are similar to that at  $T < 1100$  °C when H<sub>2</sub>O is <1%, and NO emission increases as the H<sub>2</sub>O increases but decreases with temperature when the H<sub>2</sub>O concentration is >1%.

In the absence of H<sub>2</sub>O, NO is reduced to N<sub>2</sub> by the direct CO oxidation. In the presence of H<sub>2</sub>O, the formation of free-radical H is conducive to NO reduction. At  $T < 1100$  °C, the reaction pathway of NO reduction is NO → HNO → NH → N<sub>2</sub>O → N<sub>2</sub>, the controlling factors of NO reduction are temperature and H<sub>2</sub>O content, and an increase in temperature and H<sub>2</sub>O concentration can increase the equilibrium concentrations of OH and H; H plays a great role in NO reduction path. At  $1100$  °C <  $T < 1400$  °C and [H<sub>2</sub>O] < 1.0%, the controlling factor of NO reduction is H<sub>2</sub>O concentration rather than temperature; increasing the H<sub>2</sub>O concentration makes the free-radical H content reach high equilibrium concentration; at [H<sub>2</sub>O] > 1% and  $T > 1400$  °C, NO reduction depends on the free-radical H and CO content in the reaction pathways, and NO reduction depends on the combined effects of H and CO.

## ■ AUTHOR INFORMATION

### Corresponding Author

\*Tel.: +8610-82544231. Fax: +86 10 82544231. E-mail: lisen@imechac.cn.

### Notes

The authors declare no competing financial interest.

## ■ ACKNOWLEDGMENTS

Financial support by National Natural Science Foundation of China (No. 50976123) and the Knowledge Innovation Program of the Chinese Academy of Sciences (No. KG CX2-YW-321) is acknowledged.

## ■ REFERENCES

- (1) Khopkar, S. M. *Environmental Pollution Monitoring and Control*; Ubs Pune, New Age International Publishers, Ltd.: New Delhi, 2005.
- (2) Ueda, A.; Haruta, M. *Gold Bull.* **1999**, *26*, 3–11.
- (3) VixGuterl, C.; Lahaye, J.; Ehrburger, P. *Fuel* **1997**, *76*, 517–520.
- (4) Li, S. Y.; Wu, C. T.; Li, H. Q.; Li, B. L. *React. Kinet. Catal. Lett.* **2000**, *69*, 105–113.
- (5) Reddy, B. V.; Khanna, S. N. *Phys. Rev. Lett.* **2004**, *93*, 68301–68304.
- (6) Glarborg, P.; Kubel, D.; Kristensen, P. G.; Hansen, J.; Dam-Johansen, K. *Combust. Sci. Technol.* **1995**, *111*, 461–485.

- (7) Glarborg, P.; Kristensen, P. G.; Dam-Johansen, K.; Alzueta, M. U.; Millera, A.; Bilbao, R. *Energy Fuels* **2000**, *14*, 828–838.
- (8) Rasmussen, C. L.; Hansen, J.; Marshall, P.; Glarborg, P. *Int. J. Chem. Kinet.* **2008**, *40*, 454–480.
- (9) Mueller, M. A.; Yetter, R. A.; Dryer, F. L. *Int. J. Chem. Kinet.* **1999**, *31*, 705–724.
- (10) Musgrave, F. F.; Hinshelwood, C. N. *J. Chem. Soc.* **1933**, 56–59.
- (11) Goodwin, D. *Cantera*; Available via the Internet at <http://www.cantera.org>.
- (12) Law, C. K. *Proc. Combust. Inst.* **2007**, *31*, 1–29.
- (13) Schlichting, H.; Gersten, K. *Boundary Layer Theory*; Springer-Verlag: New York, 2000.
- (14) Smith, G. P.; Golden, D. M. Available via the Internet at <http://www.me.berkeley.edu/grimech/>.
- (15) Som, S.; Ramírez, A. I.; Hagerdorn, J.; Saveliev, A.; Aggarwal, S. K. *Fuel* **2008**, *87*, 319–334.
- (16) Giles, D. E.; Som, S.; Aggarwal, S. K. *Fuel* **2006**, *85*, 1729–1742.
- (17) Kim, J. S.; Park, J.; Bae, D. S.; Vu, T. M.; Ha, J. S.; Kim, T. K. *Int. J. Hydrogen Energy* **2010**, *35*, 1390–400.
- (18) Li, S.; Wei, X. L.; Yu, L. X. *Appl. Energy* **2011**, *88*, 1113–1119.
- (19) Li, S.; Wei, X. L. *Energy Fuels* **2011**, *25*, 3465–3475.